

## LIQUID DISPLACEMENT DURING OILWELL CEMENTING OPERATIONS

Eduardo S.S. Dutra<sup>1</sup>, Mônica F. Naccache<sup>1</sup>, Paulo R. Souza Mendes<sup>1</sup>  
Cristiane R. Miranda<sup>2</sup>, André L. Martins<sup>2</sup>, Gilson Campos<sup>2</sup>

<sup>1</sup> Pontifícia Universidade Católica-RJ, RJ 22453-900, Rio de Janeiro, Brazil.

<sup>2</sup> PETROBRAS, Rio de Janeiro, Brazil.

### ABSTRACT

In oilwell primary cementing and side track / abandonment plug operations, fluid substitution is a major issue. In such operations, the drilling fluid is often displaced by wash and spacer fluids and finally by the cement slurry. The displacement quality is controlled by the interface shape between the two fluids: sharp profiles tend to result in fluid channeling, while flat profiles normally promote efficient displacement. Due to the chemical incompatibility between the oil based drilling fluid and the cement slurry, their contact can result in severe operational problems. The optimization of the fluid rheological properties is essential for the success of such operations. This fact motivated an experimental and theoretical research effort aiming at the displacement optimization in eccentric annular gaps. Large scale experiments plus Computational Fluid Dynamics (CFD) simulation analysis are performed in order to understand the parameters governing the displacement mechanics. The experimental results are not yet available. As a result of the CFD analysis, guidelines concerning fluid flow rates, volumes, densities and rheological properties are provided both for primary cementing and side track / abandonment plug operations.

### INTRODUCTION

During drilling operation of oil wells, drilling muds should lubricate and cool the drill, and remove the produced drilling cuts. After this process, it should be removed and replaced by a cement paste, which should provide the well integrity after the cement solidification (cure time). An oil well lifetime is strongly influenced by the cementing operation. In this process, the cement pushes the drilling mud in a laminar or turbulent flow, through an eccentric annular space between the rock formation and the casing. A perfect operation is when all of drilling mud is removed. It is worth noting that it is very important to avoid the contamination of the cement by the drilling mud, in order to prevent from the lost of the desirable cement properties. Therefore, some intermediate fluids, called washing or spacer fluids, are inserted between them. These fluids typically are a mixture of water and detergents, and behave as Newtonian fluids, while drilling muds and cement pastes are typically highly non-Newtonian in nature.

The interface shape between these fluids plays a crucial role during the flow. For a better displacement, the interface shape should be as flat as possible. Sharp interfaces are associated to a channeling phenomenon, where the displacer fluid crosses the displaced one, making the process very inefficient. This undesirable phenomenon may be due to the viscosities

ratio or densities differences between the fluids, non-symmetric velocity profile (in the eccentric situations) or flow regime.

Some works (Haut e Crook, 1979; Haut e Crook, 1981; Sauer, 1987; Lockyear e Hibbert, 1989) show that the process of fluid displacement through vertical oil wells are mainly governed by the viscosity ratio between fluids, the eccentricity of annular space between the column and the casing, the flow rate and the densities ratio. Jakobsen et al. (1991) analyzed experimentally the effects of viscosities ratio, buoyancy force and turbulence intensity in mud displacement through an eccentric annular tube. The results obtained show that displacement is more efficient at the largest region, and that turbulence reduces the mud channeling at the narrowest region of the flow. Tehrani et al. (1992) performed a theoretical and experimental study of laminar flow of drilling fluids through eccentric annular spaces. They observed that as the eccentricity increases, the displacement becomes worse. For vertical displacements, it is also showed that the process is more efficient for higher densities differences between the displacer (higher density) and displaced fluids. Vefring et al. (1997) analyzed numerical and experimentally, the influence of rheological and flow parameters in the displacement of a drilling mud followed by a cement paste. The results obtained indicate that numerical simulations provide good results in this kind of problems. Frigaard et al. (2002 e 2003) present some theoretical results of cement displacement through eccentric annuli, considering a two dimensional situation. They show that the displacement front may reach permanent regime for some combinations of physical properties. For these cases, an analytical expression for the interface shape is obtained.

Guillot et al. (1990) performed a theoretical approximate analysis of the flow of a washing fluid pushing a drilling mud through eccentric annuli. All the results

were obtained with the washing fluid density greater than the mud density, and they concluded that turbulent flows present smoother interface shapes than the laminar ones.

The main goal of present work is to analyze numerically the tri-dimensional flow of a washing fluid pushing a drilling mud and a cement paste pushing a spacer fluid. The numerical solution of the conservation equations is obtained via the finite volume technique. The effects of flow rate and eccentricity in the interface shape are investigated.

## NUMERICAL MODELING

The numerical solution of the flow was obtained via the finite volume technique and the volume of fluid method (VOF), using the Fluent Software (Fluent Inc., 2003). The VOF method solves a set of mass conservation equations and obtains the volume fraction of each phase  $\alpha_j$  through the domain, which should sum up unity inside each control volume. Therefore, if

$\alpha_i=0$ , the volume does not contain the phase  $j$ ;

$\alpha_i=1$ , the volume contains only the phase  $j$ ;

$0 < \alpha_i < 1$ , the volume contains the interface.

In this study, only two phases are present. The properties appearing in the transport equations  $\varphi$ , are given by:

$$\varphi = \alpha_2 \varphi_2 + (1 - \alpha_2) \varphi_1 \quad (1)$$

The interface between phases is obtained by the solution of continuity equation for  $\alpha_j$ :

$$\frac{\partial \alpha_j}{\partial t} + u_i \frac{\partial \alpha_j}{\partial x_j} = 0 \quad (2)$$

The volume fraction of the other phase is obtained with the following constraint equation:

$$(\alpha_1 + \alpha_2) = 1 \quad (3)$$

The momentum equation is given by:

$$\frac{\partial(\rho u_i)}{\partial t} + \frac{\partial(\rho u_i u_k)}{\partial x_i} = -\frac{\partial P}{\partial x_k} + \frac{\partial}{\partial u_i} \left[ \eta \left( \frac{\partial u_i}{\partial x_k} + \frac{\partial u_k}{\partial x_i} \right) \right] + \rho g_k \quad (4)$$

In the above equation,  $x_i$  are the coordinates,  $u_i$  are the velocity components,  $P$  is the pressure,  $\rho$  is the density and  $\eta$  is the viscosity function.

## METHODOLOGY

The numerical solution was obtained for two different situations. The first one corresponds to the cases where drilling mud is displaced by a washing fluid, while the other one considers that cement paste pushes the spacer fluid. It is worth noting that drilling mud and cement paste are both non-Newtonian fluids. Therefore, it is very important to have their viscosities, which are functions of the deformation rate, well determined. The relation between densities also has a significant effect on the displacement performance. When the displaced fluid is denser than the displacer fluid, buoyancy forces may help to generate the channeling phenomenon.

All cases analyzed were based on petroleum industry real data, considering equivalent dimensionless numbers. The mean entrance velocity of the displacer fluid is obtained by measured Reynolds number. The Reynolds number is given by:

$$Re = \frac{\rho v D_h}{\eta_c} \quad (5)$$

where  $v$  is the mean entrance velocity,  $\rho$  is the density,  $D_h$  is the hydraulic diameter (= difference between outer and inner tube diameters) and  $\eta_c$  is the characteristic viscosity, evaluated at a characteristic deformation rate, given by:

$$\dot{\gamma}_c = \frac{2v}{D_h} \quad (6)$$

A mean entrance velocity equal to 0.1524 m/s for the numerical simulation was obtained for the case that corresponds to a real flow rate equal to one barrel per minute (1 bpm). For the maximum real flow rate, the mean entrance velocity is 1.524 m/s. The tube length was considered equal to 2m. After extensive mesh tests, it was chosen a mesh with 100 control volumes in axial direction, 20 control volumes in radial direction and 20 control volumes in angular direction (100x.20x20) The velocity results and the interface shape obtained with this mesh were compared to the ones obtained with a 200x20x20 mesh, a 400x20x20 mesh and a 200x40x20 mesh. The differences on velocity values were below 0,1 %, and the interface shape was almost the same for these four cases.

The eccentricity using the STO concept is defined in figure 1, where  $C$  is the gap between inner and outer cylinders,  $A$  is the outer cylinder diameter, equal to 92 mm, and  $B$  is the inner cylinder diameter, equal to 42 mm. All results were obtained for  $STO = 0$  (maximum eccentricity); 0.25; 0.75 and 1 (concentric cylinders).

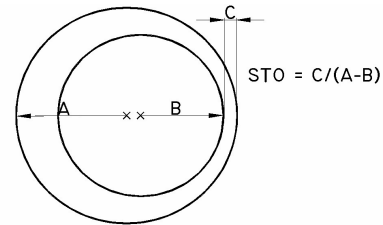


**Figure 1:** Top view of annular space

Another important dimensionless parameter is the viscosity ratio  $RV = \mu_2 / \mu_1$ , where  $\mu_1$  e  $\mu_2$  are the characteristic viscosities of displaced and displacer fluids, respectively.

Several tests were performed for the rheological characterization of real fluids (mud and cement). The rheological properties were obtained using the rotational

rheometer “Advanced Rheometric Expansion System” (ARES, Rheometric Scientific), with cone-and-plate geometry, 50 mm diameter and a gap equal to 0.2 mm. The results obtained are shown in figs. 2 and 3.

Using the previous experimental data, the mud viscosity is modeled by the Power-Law equation and the cement viscosity is best fitted by the Herschel-Bulkley equation. Then, the rheological parameters obtained are used as input data for the numerical simulations.

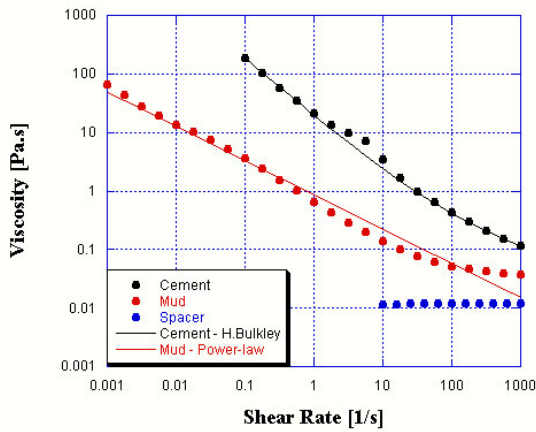


**Figure 2:** Viscosity function for drilling mud, cement paste and washing fluid

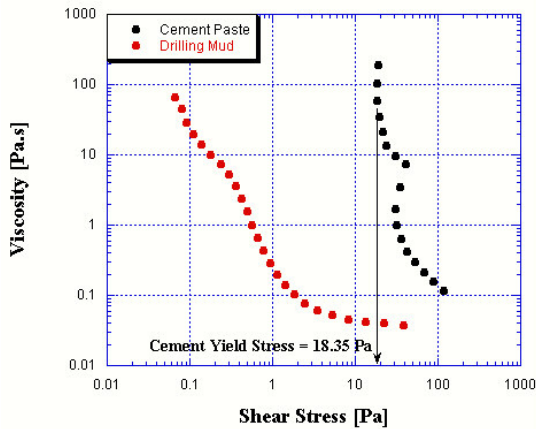


**Figure 3:** Drilling mud and cement paste viscosities as functions of shear stress.

Viscosity functions

The Power-Law model is given by:

$$\eta = K\dot{\gamma}^{n-1} \quad (7)$$

where  $K$  is the consistency index,  $n$  is the Power-Law exponent,  $\dot{\gamma} = \sqrt{1/2 \text{tr} \dot{\underline{\underline{\gamma}}}}^2$  is the deformation rate modulus, and  $\dot{\underline{\underline{\gamma}}} = (\nabla \underline{u} + \nabla \underline{u}^T)$  is the rate-of-deformation tensor.

In order to avoid numerical problems, the software uses a truncated Power-Law model, defined by:

$$\begin{cases} \eta = \eta_0 & \text{if } \eta \geq \eta_0 \\ \eta = K\dot{\gamma}^{n-1} & \text{if } \eta_\infty < \eta < \eta_0 \\ \eta = \eta_\infty & \text{if } \eta \leq \eta_\infty \end{cases} \quad (8)$$

where  $\eta_\infty$  and  $\eta_0$ , are the inferior and superior viscosity limits, respectively.

The Herschel-Bulkley model is described by the equation bellow.

$$\begin{cases} \eta = \frac{\tau_0}{\dot{\gamma}} + k\dot{\gamma}^{n-1} & \text{se } \tau \geq \tau_0 \\ \eta = \infty & \text{se } \tau < \tau_0 \end{cases} \quad (9)$$

Accordingly to figure 3, when the stress modulus is lower than 18.35 Pa, the fluid has a very large viscosity, and behaves as a solid material. This critical stress is called yield stress ( $\tau_0$ ).

The following rheological parameters were obtained from the curve fitting:

Drilling mud (truncated Power-law model):  $\eta_0 = 1000$  Pa.s,  $\eta_\infty = 0.01$  Pa.s,  $K = 0.86$  Pa.s<sup>n</sup>,  $n = 0.414$ .

Cement paste (Herschel-Bulkley model):  $\tau_0 = 18.35$  Pa,  $K = 1.5$  Pa.s<sup>n</sup>,  $n = 0.6$ .

Washing and spacer fluids (Newtonian):  $\mu = 0.01$  Pa.s

The densities used were also obtained from real data:  $\rho_{\text{cement}} = 1980$  Kg/m<sup>3</sup>,  $\rho_{\text{mud}} = 1200$  Kg/m<sup>3</sup> e  $\rho_{\text{w/s}} = 1000$  Kg/m<sup>3</sup>.

The fluids are considered immiscible, and the effects of surface tension are included in the VOF model via the continuum surface force model, which is implemented by adding a source term in the momentum equation (Fluent Inc., 1996). All results are obtained with the surface tension equal to 0.02 N/m. The contact angle at wall is

defined as  $90^\circ$ . It is used to adjust the surface normal in cells near the walls. Some numerical tests were done to analyze the influence of the contact angle through the interface shape, but no changes on flow behavior were observed.

#### HEADINGS AND PARAGRAPHS

The numerical results are obtained for two configurations: the cement paste pushing the spacer fluid, and the washing fluid pushing the drilling mud. The annular geometry has two meters length ( $\vec{g} = -g_x \hat{e}_x$ ), inner diameter equal to 42 mm and outer diameter equal to 92 mm.

Two different flow rates and five eccentricities are used in numerical simulations. The Reynolds numbers were calculated by eq. (5), always using the properties of the non-Newtonian fluid in each case.

It can be observed that when the viscosities ratio is greater than one (cement pushing the spacer fluid), the displacement performance is better. In these cases, the minimum flow rate condition provides a flatter interface shape, leading to a better displacement. For the other situation, when the washing fluid pushes the drilling mud (viscosities ratio less than one), it is noted that for the maximum flow rate condition, the interface shape is as sharp as it occurs for the other configuration (spacer fluid displaced by cement). However, in these cases when flow rate decreases to 1 bpm, the drilling mud viscosity increases and its displacement becomes heavier. The densities difference also plays a role in this process. Buoyancy forces act over the mud, forcing it to move in the opposite direction. It can also be noted that these cases presented some numerical instabilities.

The effect of eccentricity is similar for all situations. The displacement tends to be more efficient through larger regions of the annular space. However, it can be noted that in the cases of minimum flow rates and washing fluids pushing the drilling mud, the

displacement is almost the same in all regions.

Below are shown the results for the four cases studied including the five eccentricities. They are shown horizontally arranged but in the simulation they were in vertical position, with the gravity opposed to the flow.

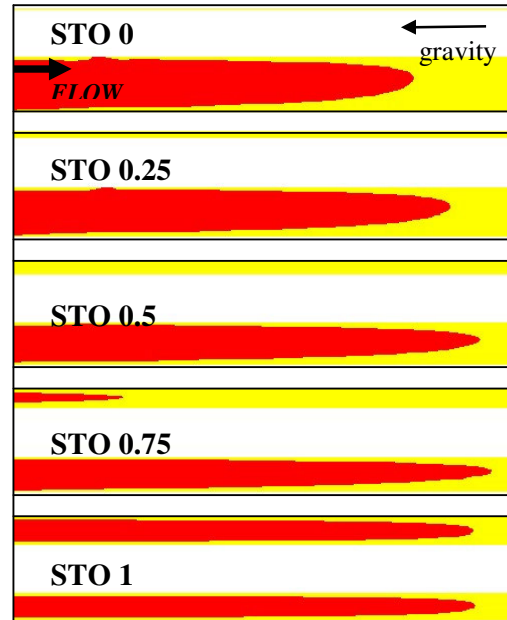


**Figure 4:** Spacer (red) displacing Mud (yellow). Maximum flow rate,  $Re = 1183$ .

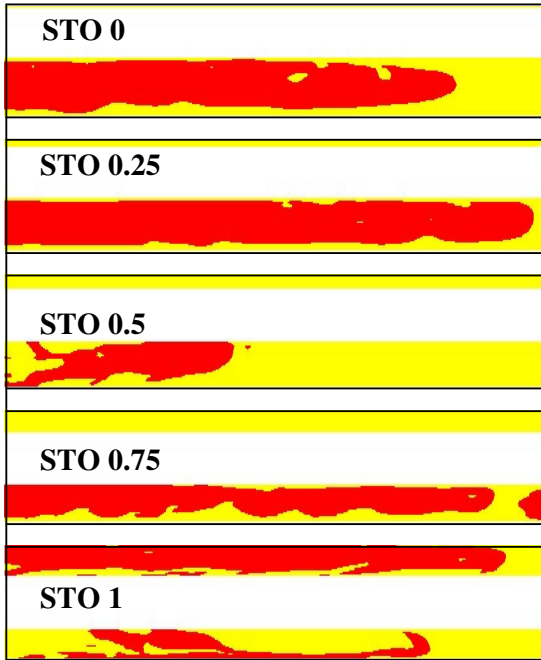


**Figure 5:** Spacer (red) displacing Mud (yellow). Minimum flow rate,  $Re= 307$ .



**Figure 7:** Cement (red) displacing Spacer (yellow). Minimum flow rate,  $Re= 4.04$ .

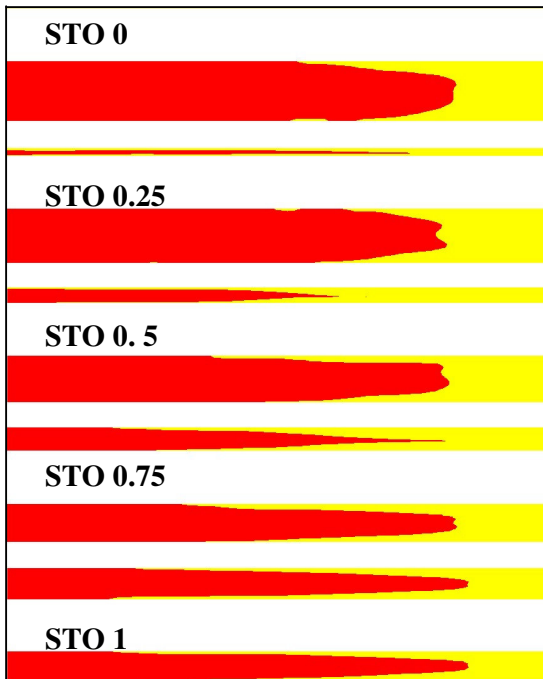


**Figure 6:** Cement (red) displacing Spacer (yellow). Maximum flow rate,  $Re= 255$ .

Another way to analyze the displacement process efficiency is evaluating the quantity of displacer fluid inside the computational domain, as a function of the normalized rate of pumped fluid, which is similar to the pumping time. It can be observed, with the aid of figs. 10 and 11, that larger slopes represent more efficient processes. It can also be observed that better performances are obtained when cement pushes the spacer fluid, because the quantity of displacer fluid inside the well reaches unity for lower times, mainly for low pump rates, when cement viscosity increases. The worst case is spacer displacing mud at low pump rates because the mud viscosity increasing. It can also be noted that the influence of eccentricity in the displacement efficiency is very small, and becomes more evident only in the cases where the drilling mud is displaced by the washing fluid. It can be concluded that the most efficient process could be those with the displacing fluid always the more viscous and also dense.

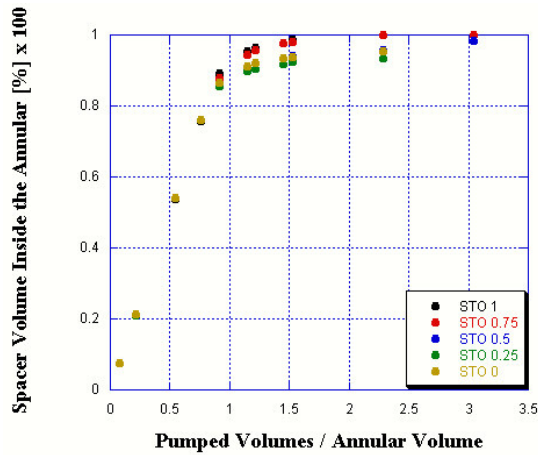


**Figure 8:** Displacement Efficiency. Spacer displacing Mud. Maximum flow rate. Re = 1183

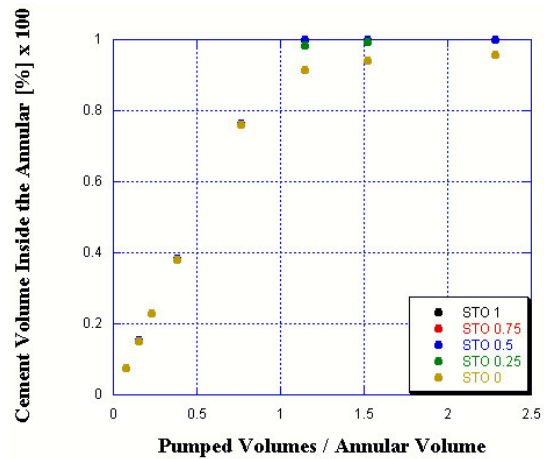


**Figure 10:** Displacement Efficiency. Cement displacing Spacer. Maximum flow rate. Re = 255

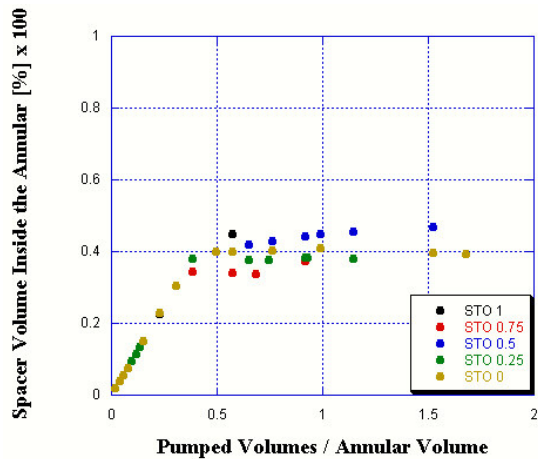


**Figure 9:** Displacement Efficiency. Spacer displacing Mud. Minimum flow rate. Re = 307

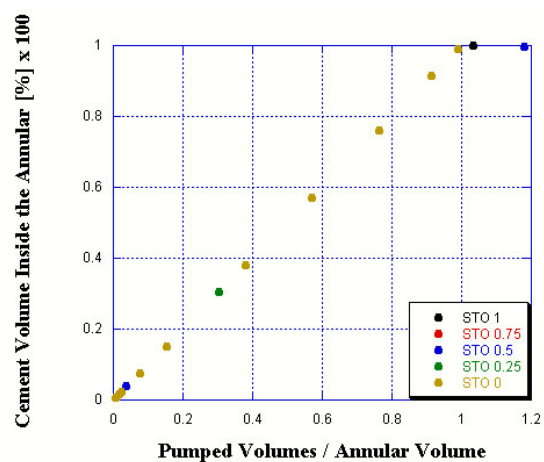


**Figure 11:** Displacement Efficiency. Cement displacing Spacer. Minimum flow rate. Re = 4.04

#### FINAL REMARKS

In this work it the displacement process of two immiscible fluids through eccentric annuli is analyzed, to investigate the cementing process in oil wells. Two different situations are investigated: a non-Newtonian fluid, with rheological properties similar to that ones of the cement paste, pushing a Newtonian fluid; and a Newtonian fluid pushing a non-Newtonian one, with

rheological properties similar to that ones of the drilling mud. The solutions are obtained numerically, via the finite volume technique and the volume of fluids method. When the viscosities ratio is greater than one, the results show that the displacement is better for smaller flow rates. Larger flow rates lead to smaller viscosities of the displacer fluid due to higher deformation rates, and the process efficiency decreases. However, when the viscosities ratio is less than one, the opposite occurs, and larger flow rates increase the process efficiency.

The influence of eccentricity on the interface shape is rather small, but a little higher efficiency is obtained with lower values of eccentricity.

#### ACKNOWLEDGMENTS

Financial support for the present research was provided by Petrobras, CNPq and MCT.

#### REFERENCES

1. Barnes, H. A., 2000, "A Handbook of Elementary Rheology", The University of Wales.
2. Bird, R. B., Armstrong, R. C., Hassanger O., 1987, "Dynamics of Polymeric Liquids", vol. 1, Wiley, 1987.
3. Fluent User's Guide, version 6.1, Fluent Inc., 2003.
4. Frigaard I. A., Bittleston S. H., Ferguson J., 2002 – "Mud Removal and Cement Placement During Primary Cementing of an Oil Well" – Society of Petroleum Engineers – Kluwer Academic Publishers.
5. Frigaard I. A., Pelipenko S., 2003 – "Effective and Ineffective Strategies for Mud Removal and Cement Slurry Design" – Society of Petroleum Engineers – (SPE) #80999.
6. Guillot D., Couturier M., Hendriks H., Callet F., 1990 – "Design Rules and Associated Spacer Properties for Optimal Mud Removal in Eccentric Annuli" – Society of Petroleum Engineers – (SPE) #21594.
7. Haut, R. C., Crook, R. J., 1979 – "Primary Cementing: The Mud Displacement Process" – Society of Petroleum Engineers – (SPE) #8253.
8. Haut, R. C., Crook, R. J., 1981 – "Laboratory Investigation of Lightweight, Low-Viscosity Cementing Spacer Fluids" – Society of Petroleum Engineers – (SPE) #10305.
9. Jakobsen J., Sterri N., Saasen A., Aas B., Kjosnes I., Vigen A., 1991 – "Displacement in Eccentric Annuli During Primary Cementing in Deviated Wells" – Society of Petroleum Engineers – (SPE) #21686.
10. Lockyear, C. F., Hibbert, A. P., 1989 – "Integrated Primary Cementing Study Defines Key Factors for Field Success" – Society of Petroleum Engineers – (SPE) #18376.
11. Macosko, C. W., 1994, "Rheology Principles, Measurements, and Applications", Wiley-VCH.
12. Sauer, C. W., 1987 – "Mud Displacement During Cementing: A State of the Art" – Society of Petroleum Engineers – (SPE) #14197.
13. Tehrani A., Ferguson J., Bittleston S.H., 1992 – "Laminar Displacement in Annuli: A Combined Experimental and Theoretical Study" – Society of Petroleum Engineers – (SPE) #24569.
14. Vefring E. H., Bjorkevoll K. S., Hansen S. A., Sterri N., Saevareid O., Aas B., Merlo A., 1997 – "Optimization of Displacement Efficiency During Primary Cementing" – Society of Petroleum Engineers – (SPE) #39009.